Electronic Supplementary Information (ESI)

Modulation on Terahertz Absorption Properties in Ln^{III}-$[Ag^{I}(CN)_2]$ Networks

Guanping Li, [a,c] Olaf Stefanczyk,*[a] Kunal Kumar, [a] Yuuki Mineo, [a] Lidong Wang, [a] Koji Nakabayashi, [a] Marie Yoshikiyo, [a] Nicholas F. Chilton, [c,d] and Shin-ichi Ohkoshi*[a,b]

[a]*Department of Chemistry, School of Science, The University of Tokyo, 7-3-1 Hongo, Bunkyo-ku, Tokyo 113-0033, Japan*

[b]*DYNACOM (Dynamical Control of Materials) - IRL2015, CNRS, The University of Tokyo, 7-3-1 Hongo, Bunkyo-ku, Tokyo 113-0033, Japan*

[c]*Department of Chemistry, The University of Manchester, Manchester, M13 9PL, U.K.*

[d]*Research School of Chemistry, The Australian National University, Canberra, ACT, 2601, Australia*

E-mails: olaf@chem.s.u-tokyo.ac.jp, ohkoshi@chem.s.u-tokyo.ac.jp

Table of contents

Section 1. Legends for Supporting Movie 2
Section 2. Single Crystal X-ray Diffraction Analyses 3
Section 3. Thermogravimetric Analysis 7
Section 4. Powder X-ray Diffraction (PXRD) Studies 8
Section 5. Solid-state UV-Vis-NIR Absorption and Vibrational Spectroscopies 9
Section 6. THz Time-domain Spectroscopy (THz-TDS) 12
Section 7. First-principles Phonon Mode Calculation 19

Section 1. Legends for Supporting Movie

Movie S1. Calculated phonon modes of LaAg and DyAg. The movie shows the atomic movements of the phonon modes for 1.024 THz (*a*-6) and 1.095 THz (*b*-4) in two different directions.

Section 2. Single Crystal X-ray Diffraction Analyses

Table S1. Crystal data, data collection, and refined parameters of **LaAg** and **DyAg**.

Compound	LaAg	DyAg
Empirical formula	$C_6H_6Ag_3LaN_6O_3$	$C_6H_6Ag_3DyN_6O_3$
Formula weight ($g\cdot mol^{-1}$)	672.69	696.28
Temperature (K)	89.95	89.95
Crystal system	hexagonal	hexagonal
Space group	$P6_3/mcm$	$P6_3/mcm$
***a* (Å)**	6.6482(6)	6.5525(17)
***b* (Å)**	6.6482(6)	6.5525(17)
***c* (Å)**	19.0910(8)	18.510(4)
α (°)	90	90
β (°)	90	90
γ (°)	120	120
***V* ($Å^3$)**	730.75(13)	688.3(4)
Z	2	2
ρ_{calc} ($g\cdot cm^{-3}$)	3.057	3.360
μ (mm^{-1})	6.834	9.580
***F* (000)**	612.0	630.0
2Θ range for data collection (°)	7.078 to 54.692	7.182 to 54.888
Index ranges	$-8 \le h \le 8$, $-8 \le k \le 8$, $-24 \le l \le 24$	$-7 \le h \le 8$, $-8 \le k \le 8$, $-24 \le l \le 24$
Reflections collected	6232	5036
Independent reflections	335 [R_{int} = 0.0262, R_{sigma} = 0.0108]	309 [R_{int} = 0.0312, R_{sigma} = 0.0143]
Data / restraints / parameters	335/6/25	309/6/27
GOF on F^2	1.419	1.290
Final *R* indexes [I>=2σ (I)]	R_1 = 0.0389, wR_2 = 0.0648	R_1 = 0.0265, wR_2 = 0.0427
Final *R* indexes [all data]	R_1 = 0.0389, wR_2 = 0.0648	R_1 = 0.0300, wR_2 = 0.0435
Largest diff. peak / hole ($e\cdot Å^{-3}$)	2.37/-1.54	2.30/-1.07
CCDC numbers	2339311	2339312

Table S2. Selected bond distances of **LaAg** and **DyAg**.

Bond distance (Å)	LaAg	DyAg
Ln1-O1	2.529(9)	2.414(7)
Ln1-O1[1]	2.529(9)	2.414(7)
Ln1-O1[2]	2.529(9)	2.414(7)
Ln1-N1	2.653(7)	2.505(5)
Ln1-N1[1]	2.653(7)	2.505(5)
Ln1-N1[2]	2.653(7)	2.505(5)
Ln1-N1[3]	2.653(7)	2.505(5)
Ln1-N1[4]	2.653(7)	2.505(5)
Ln1-N1[5]	2.653(7)	2.505(5)
Ag1-Ag1	3.3241(3)	3.2762(8)
Ag1-Ag1[6]	3.3241(3)	3.2762(8)
Ag1-Ag1[7]	3.3241(3)	3.2762(8)
Ag1-Ag1[8]	3.3241(3)	3.2762(8)
Ag1-C1[9]	2.071(8)	2.059(6)
Ag1-C1[10]	2.071(8)	2.059(6)
N1-C1	1.141(11)	1.146(9)

[1]-Y,+X-Y,+Z; [2]+Y-X,-X,3/2-Z; [3]+Y-X,-X,+Z; [4]-Y,+X-Y,3/2-Z; [5]+X,+Y,3/2-Z; [6]1-Y,+X-Y,+Z; [7]+Y-X,1-X,+Z; [8]1+Y-X,1-X,+Z; [9]1-Y,1+X-Y,+Z;

[10]1-X,1-Y,1-Z

Table S3. Selected bond angles of **LaAg** and **DyAg**.

Bond angles (°)	LaAg	DyAg
O1-Ln1-O1[1]	120.000(2)	120.000(2)
O1-Ln1-O1[2]	120.000(2)	120.000(2)
O1[1]-Ln1-O1[2]	120.000(3)	120.000(6)
Ln1-N1-C1	164.5(6)	166.4(5)
Ag1-C1-N1	178.7(8)	179.8(8)
C1-Ag1-C1[6]	180.0(9)	180.0
N1-Ln1-N1[1]	72.3(2)	72.40(19)
N1-Ln1-N1[3]	72.3(2)	72.40(19)
N1[1]-Ln1-N1[3]	72.3(2)	72.40(19)
N1[2]-Ln1-N1[5]	72.3(2)	72.40(19)
N1[2]-Ln1-N1[4]	72.3(2)	72.40(19)
N1[4]-Ln1-N1[5]	72.3(2)	72.40(19)
N1-Ln1-N1[5]	94.1(3)	94.0(2)
N1[1]-Ln1-N1[4]	94.1(3)	94.0(2)
N1[2]-Ln1-N1[3]	94.1(3)	94.0(2)
N1-Ln1-N1[2]	140.18(11)	140.13(10)
N1-Ln1-N1[4]	140.18(11)	140.13(10)
N1[1]-Ln1-N1[2]	140.18(12)	140.13(10)
N1[1]-Ln1-N1[5]	140.18(11)	140.13(10)
N1[3]-Ln1-N1[4]	140.18(12)	140.13(10)
N1[3]-Ln1-N1[5]	140.18(11)	140.13(10)

[1]-Y,+X-Y,+Z; [2]+Y-X,-X,3/2-Z; [3]+Y-X,-X,+Z; [4]-Y,+X-Y,3/2-Z; [5]+X,+Y,3/2-Z; [6]1-X,1-Y,1-Z

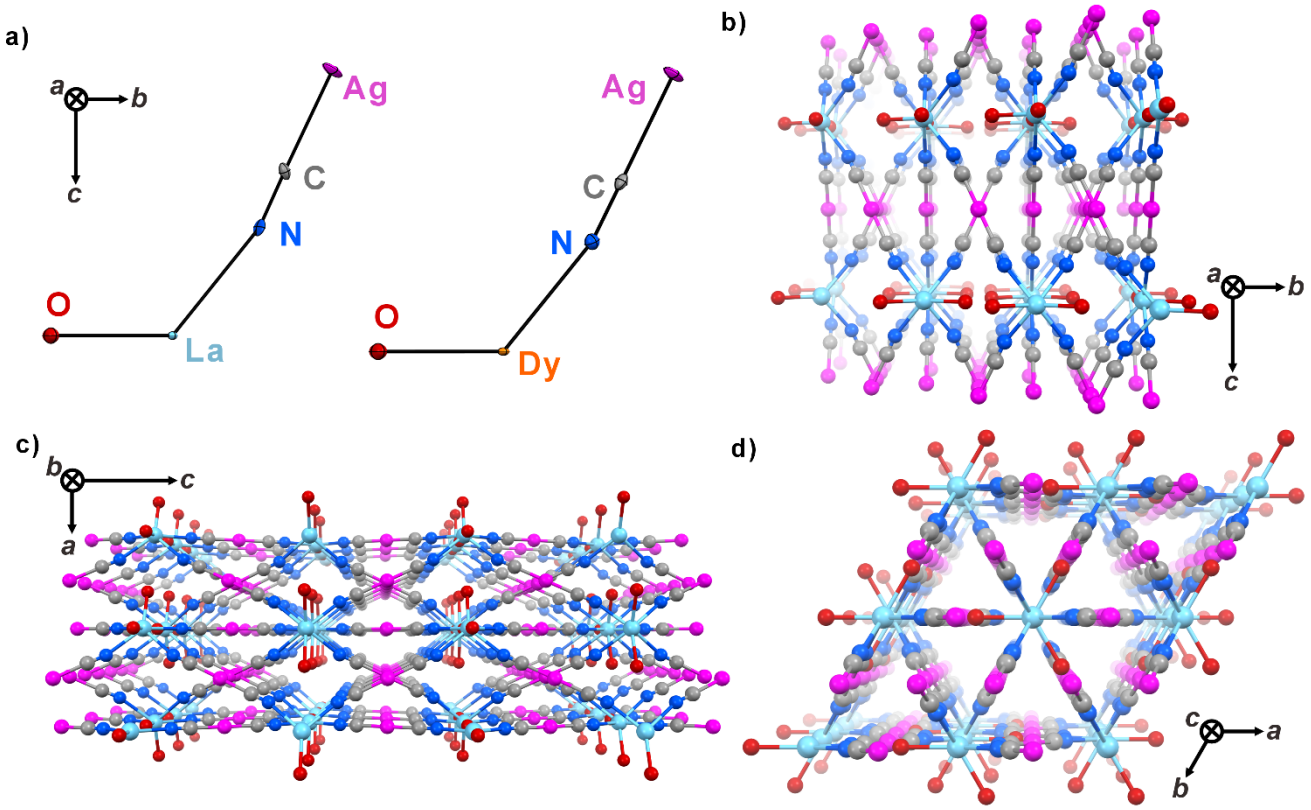

Figure S1. (a) Asymmetric units of **LaAg** (*left*) and **DyAg** (*right*) with atoms labeling along the *a*-axis measured at 90 K. Thermal ellipsoids of 50% probability are shown. Crystal packing of **LaAg** along *a*- (b), *b*- (c), and *c*- (d) crystallographic directions measured at 90 K. Color: La, cyan; Ag, pink; C, dark gray; N, blue; O, red. All hydrogens are omitted for clarity.

Section 3. Thermogravimetric Analysis

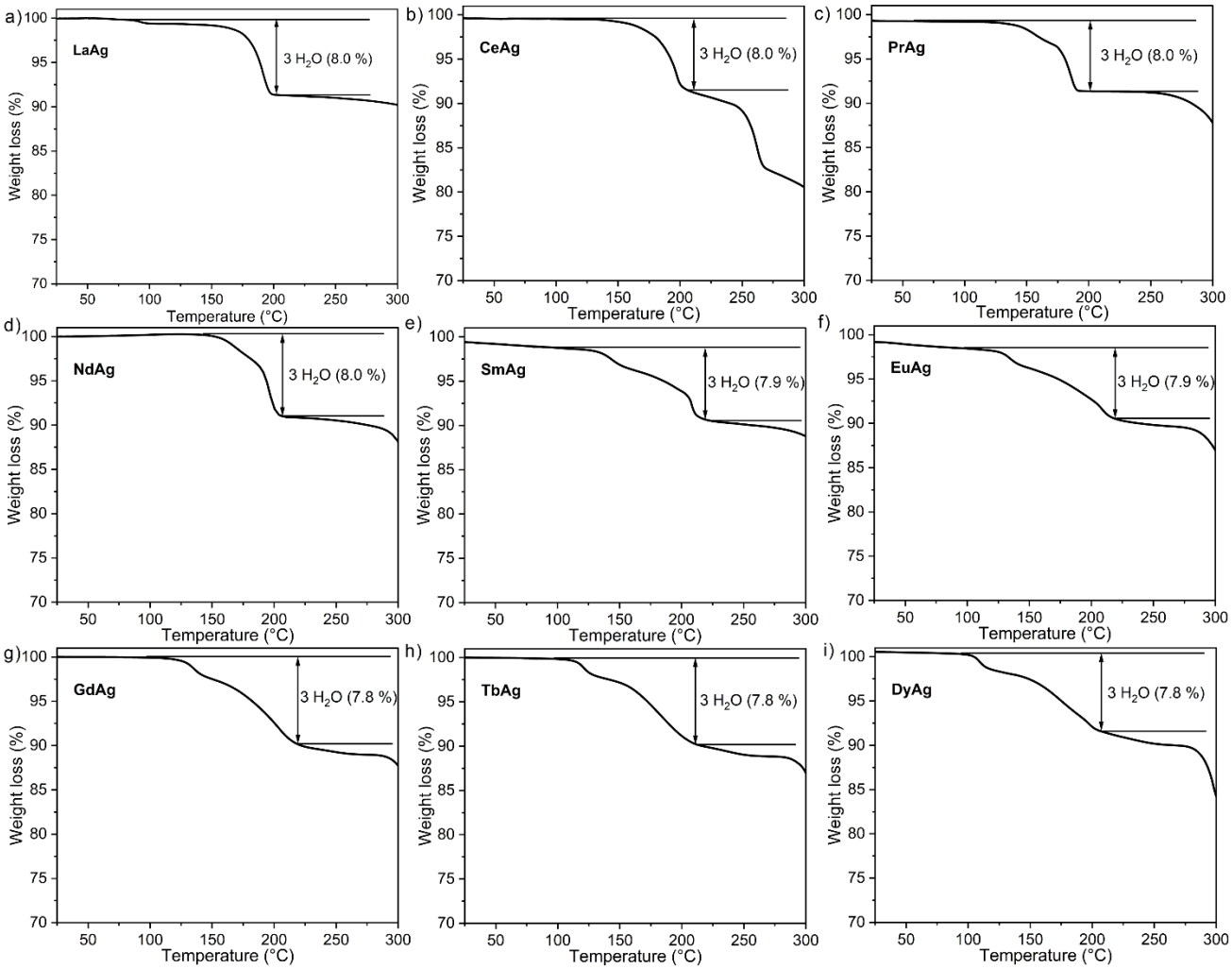

Figure S2. Thermogravimetric curves for indicated powdered samples of **LnAg**.

Section 4. Powder X-ray Diffraction (PXRD) Studies

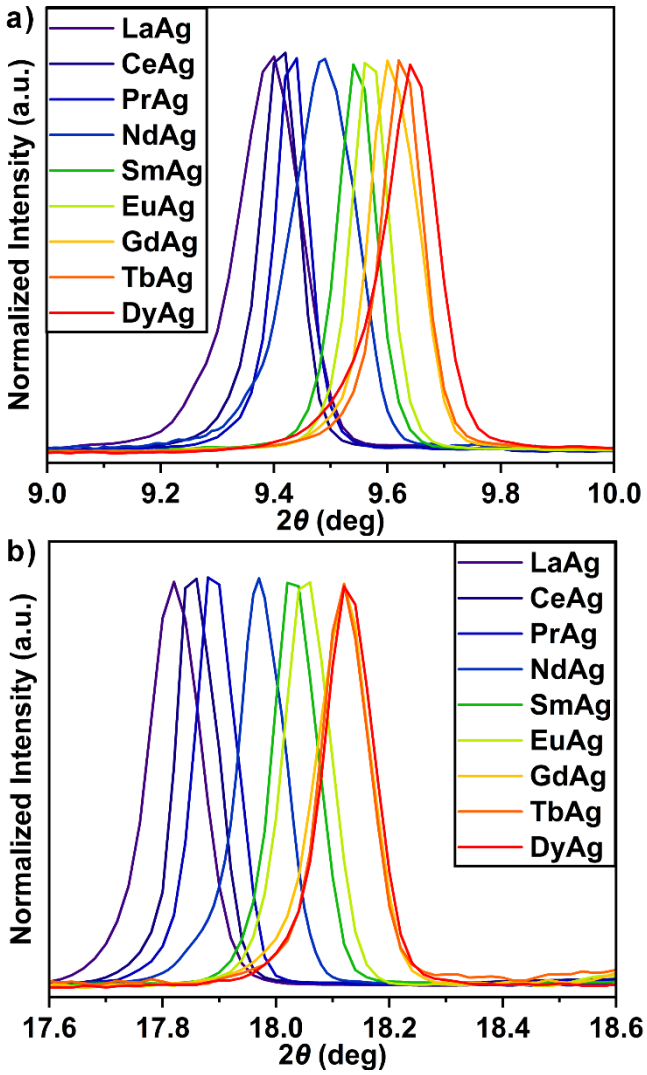

Figure S3. Experimental powder X-ray diffraction (PXRD) patterns of different **LnAg** samples in two indicated regions after normalization.

Section 5. Solid-state UV-Vis-NIR Absorption and Vibrational Spectroscopies

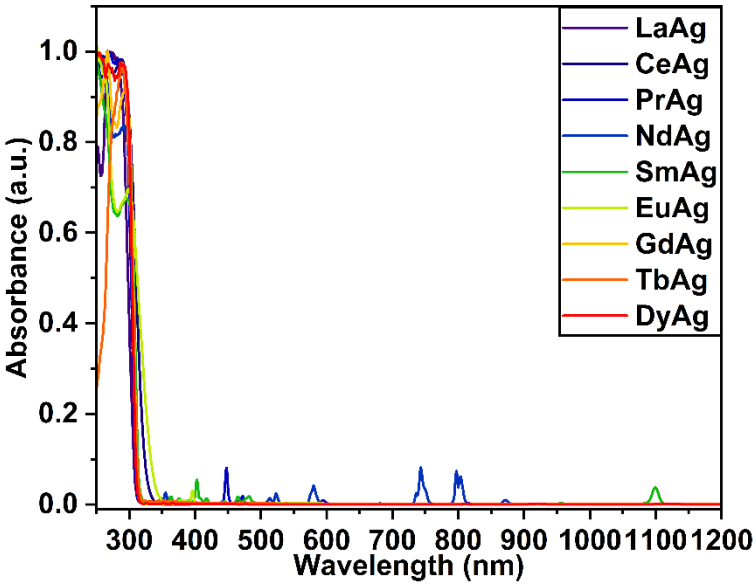

Figure S4. Normalized solid-state UV-Vis-NIR absorption spectra of different **LnAg** samples in the 250 - 1200 nm region.

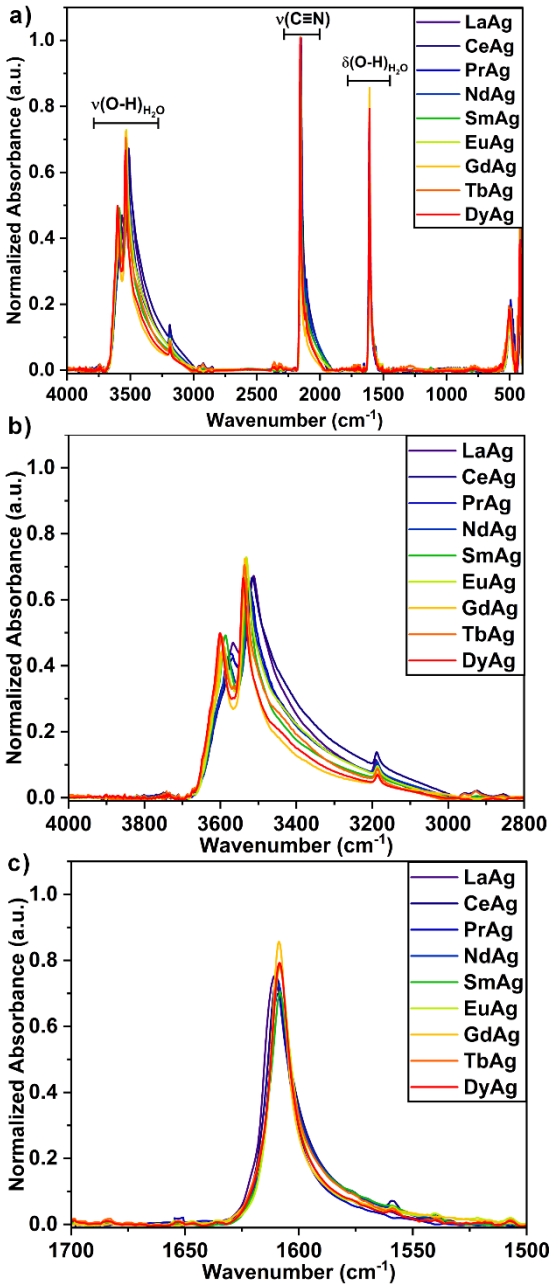

Figure S5. Normalized infrared absorption spectra of different **LnAg** samples in the 4000 - 400 cm^{-1} region (a), H_2O stretching region (b) and H_2O bending region (c).

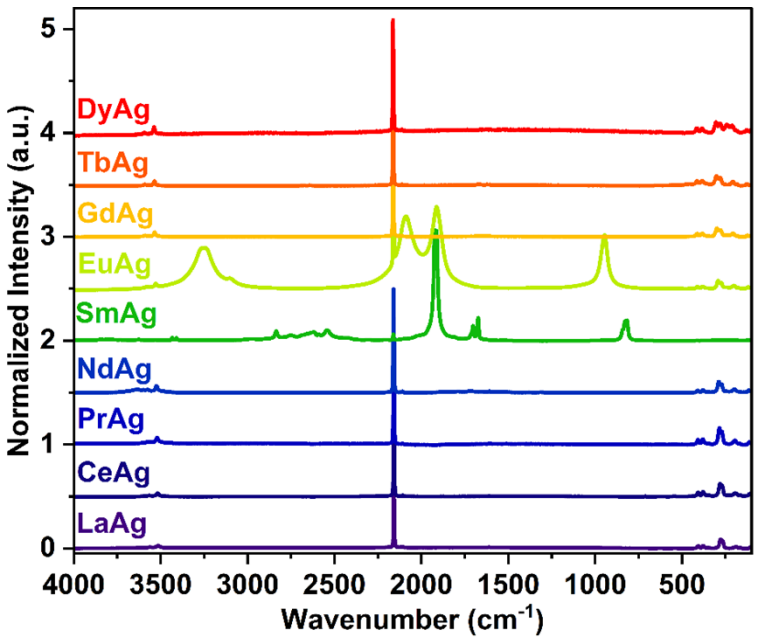

Figure S6. Normalized Raman scattering spectra of different **LnAg** samples in the 4000 - 100 cm^{-1} region.

Section 6. THz Time-domain Spectroscopy (THz-TDS)

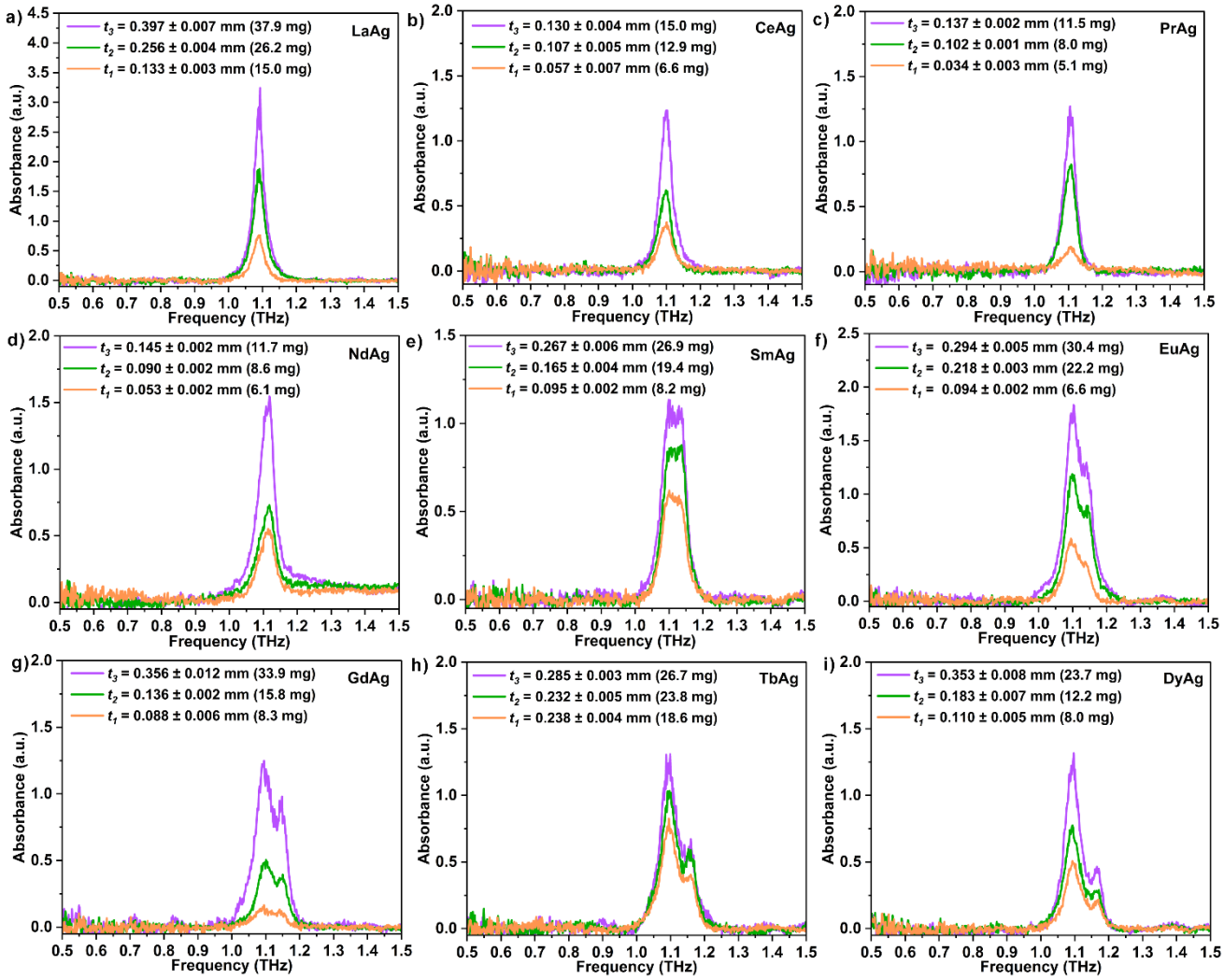

Figure S7. The room-temperature (RT) THz-TDS spectra in the 0.5 - 1.5 THz of **LnAg** pellets. The different averaged thicknesses (*t*) were calculated using thicknesses for five different positions together with standard deviations indicated in the legends. The masses for pellets were indicated in the bracket.

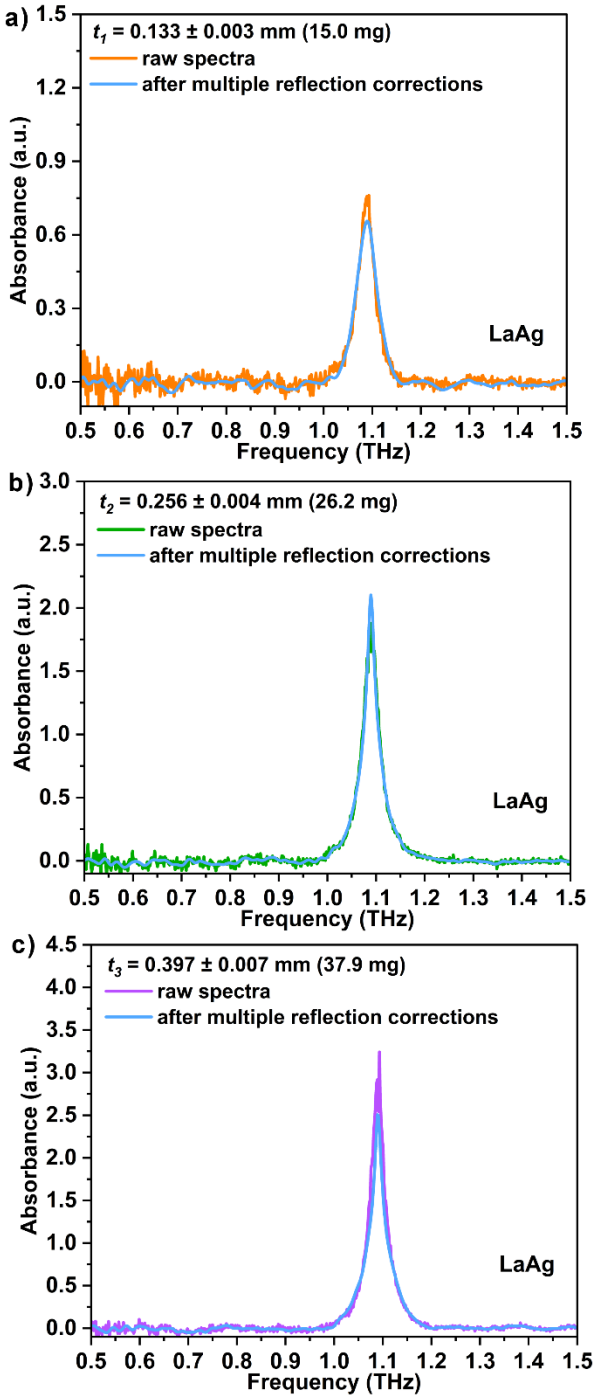

Figure S8. The RT THz-TDS spectra in the 0.5 - 1.5 THz of **LaAg** pellets in different thicknesses and masses before and after multiple reflection corrections.

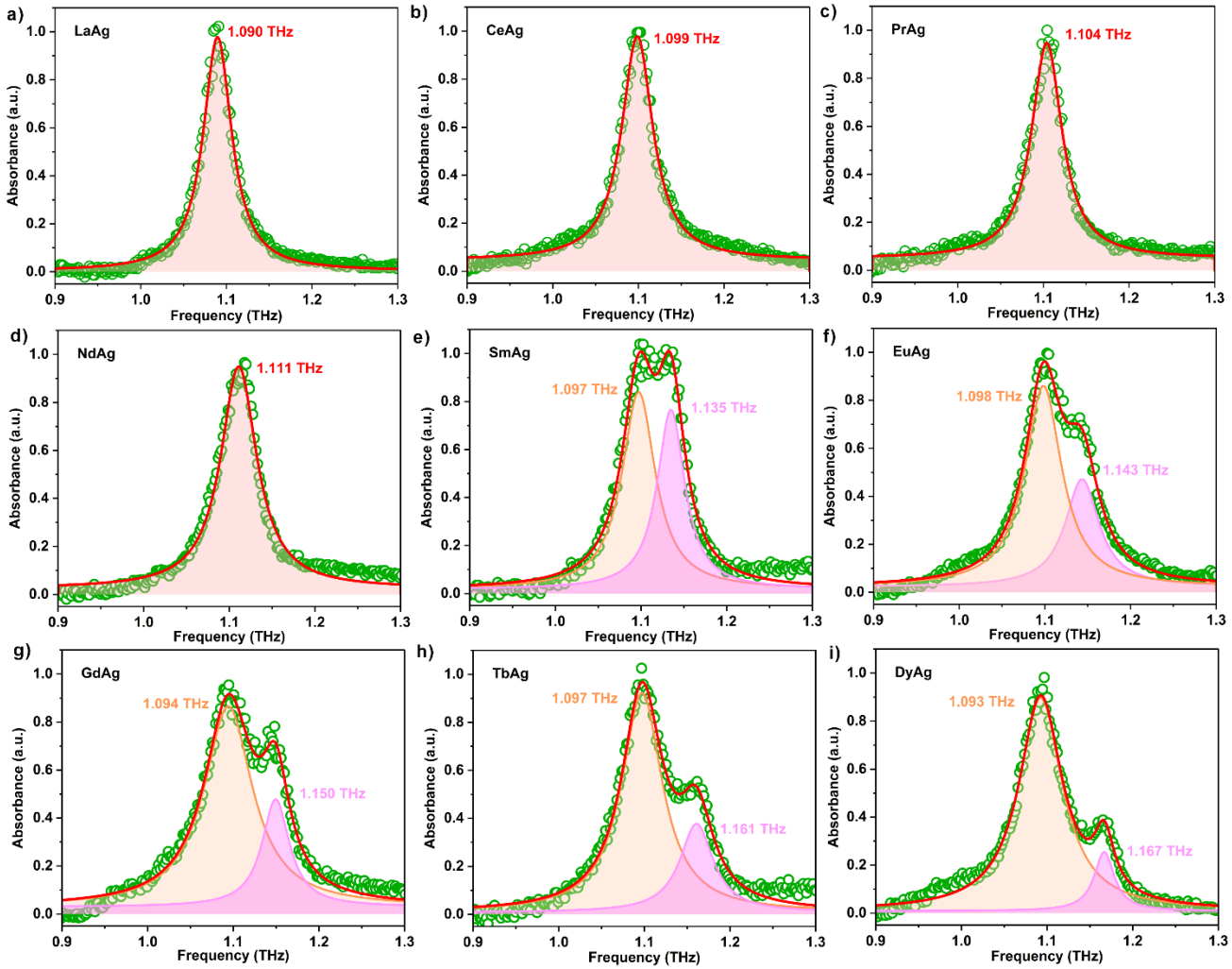

Figure S9. The normalized RT THz-TDS spectra of **LnAg** fitted with Lorentzian functions. Red lines show the fitted curves, colored peaks show the components of each peak, and green dots indicate the experimental data.

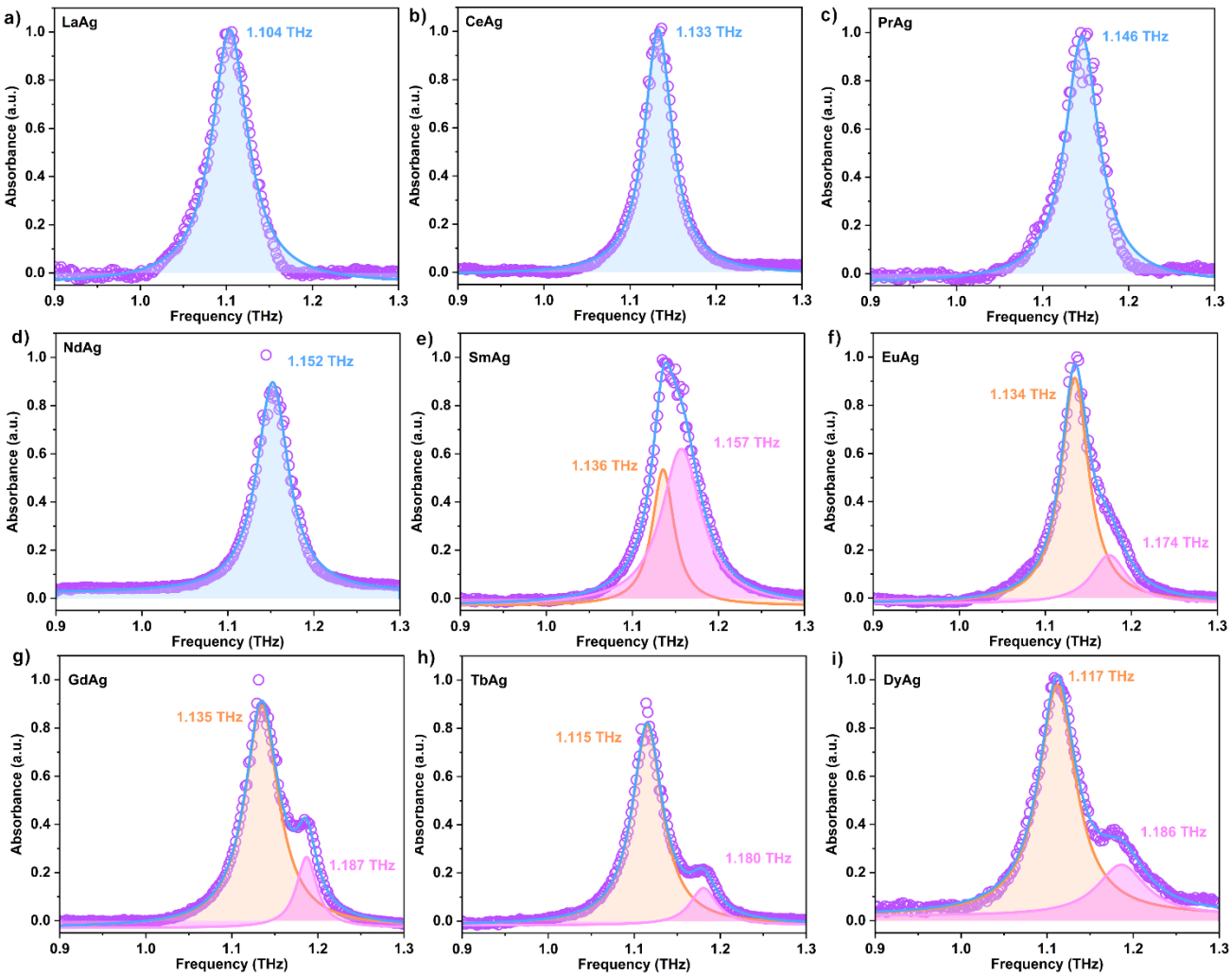

Figure S10. The normalized THz-TDS spectra at liquid nitrogen (LN) temperature of **LnAg** fitted with Lorentzian functions. Blue lines show the fitted curves, colored peaks show the components of each peak, and violet dots indicate the experimental data.

Table S4. The fitted THz absorbance spectra peak positions and full width at half maximum (FWHM) in THz for different **LnAg** samples at RT and LN temperatures. The peak shift in GHz denotes the peak position difference between RT and LN temperatures.

Compounds	Peak Position (THz)		FWHM (THz)		Peak Shift (GHz)
	RT	LN	RT	LN	
LaAg	1.090	1.104	0.082	0.102	14
CeAg	1.099	1.133	0.088	0.080	34
PrAg	1.104	1.146	0.088	0.096	42
NdAg	1.111	1.152	0.102	0.090	41
SmAg	1.135 (peak 1) 1.097 (peak 2)	1.157 (peak 1) 1.136 (peak 2)	0.078 (peak 1) 0.094 (peak 2)	0.114 (peak 1) 0.062 (peak 2)	22 (peak 1) 39 (peak 2)
EuAg	1.143 (peak 1) 1.098 (peak 2)	1.174 (peak 1) 1.134 (peak 2)	0.104 (peak 1) 0.096 (peak 2)	0.100 (peak 1) 0.078 (peak 2)	31 (peak 1) 36 (peak 2)
GdAg	1.150 (peak 1) 1.094 (peak 2)	1.187 (peak 1) 1.135 (peak 2)	0.078 (peak 1) 0.014 (peak 2)	0.058 (peak 1) 0.096 (peak 2)	37 (peak 1) 41 (peak 2)
TbAg	1.161 (peak 1) 1.097 (peak 2)	1.180 (peak 1) 1.115 (peak 2)	0.100 (peak 1) 0.270 (peak 2)	0.076 (peak 1) 0.086 (peak 2)	19 (peak 1) 18 (peak 2)
DyAg	1.167 (peak 1) 1.093(peak 2)	1.186 (peak 1) 1.117 (peak 2)	0.058 (peak 1) 0.124 (peak 2)	0.136 (peak 1) 0.104 (peak 2)	19 (peak 1) 24 (peak 2)

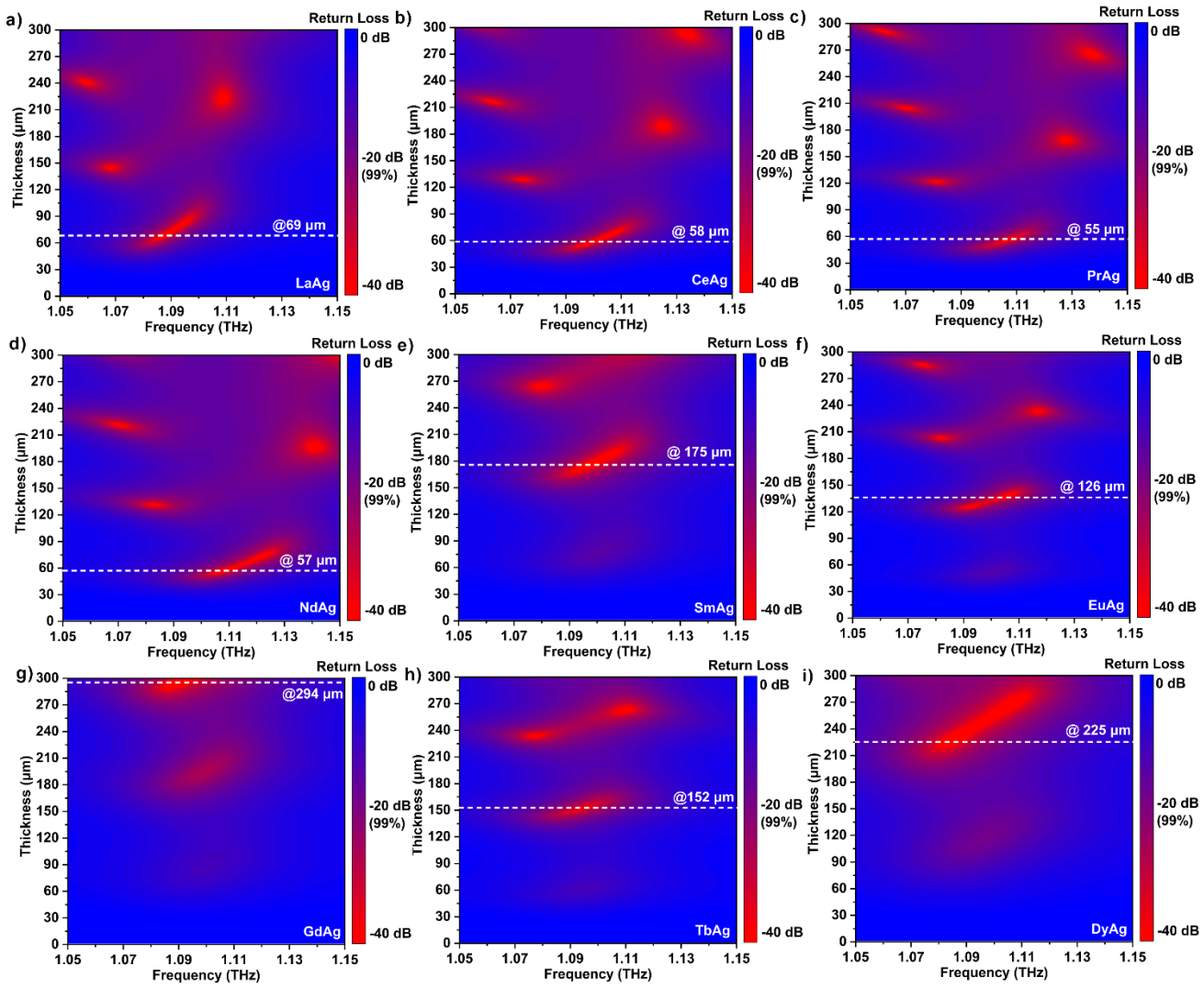

Figure S11. Colormaps depicting the return loss (*RL*) intensity in decibels (dB) as a function of frequency and thickness for indicated **LnAg** compounds derived from impedance matching simulations.

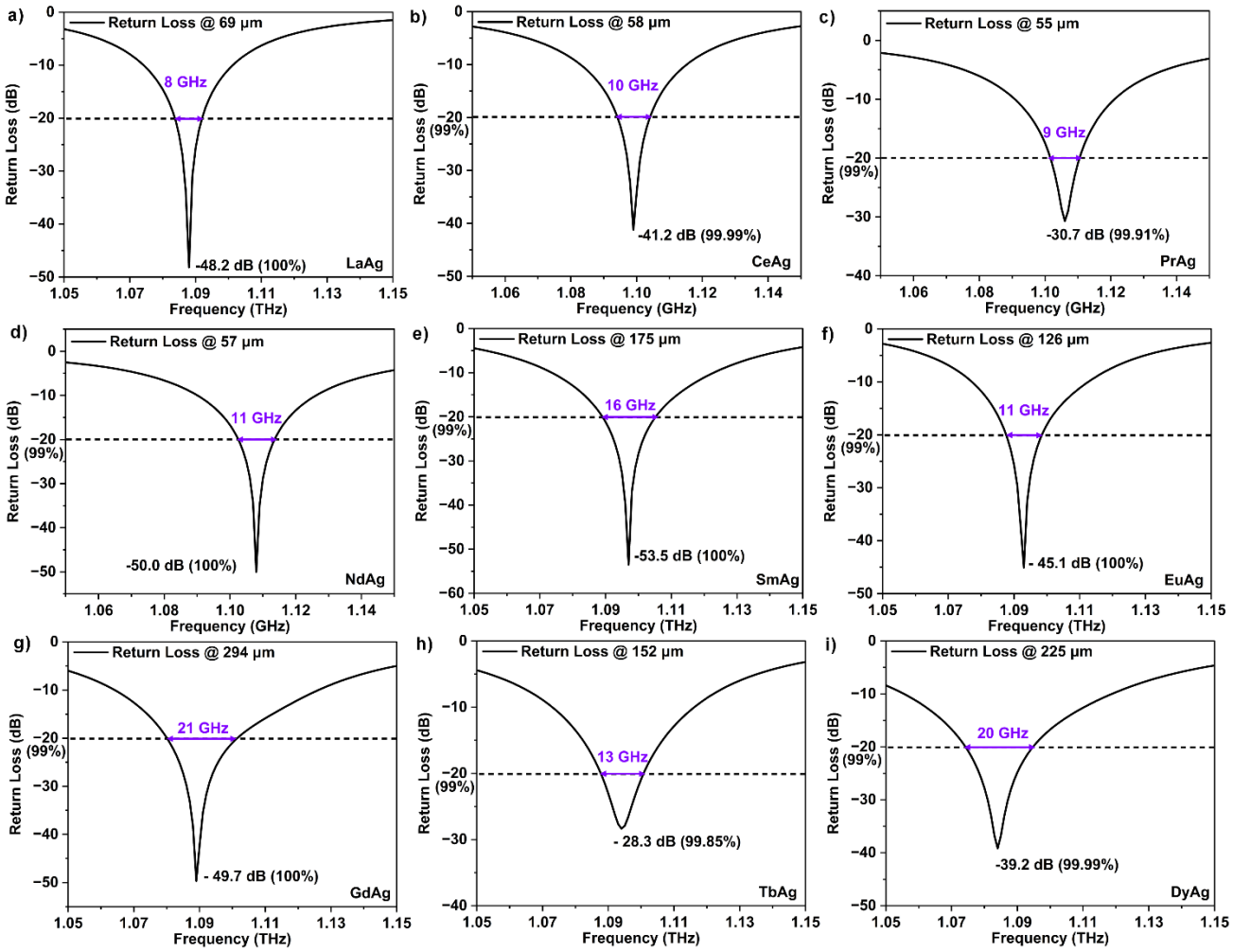

Figure S12. The calculated *RL* spectra of the **LnAg** thin films in different frequencies derived from impedance matching simulations. The violet arrows mark the effective bandwidth (GHz) at -20 dB return loss (99% absorption).

Section 7. First-principles Phonon Mode Calculation

Table S5. Calculated phonon modes obtained by first-principles phonon mode calculations of **LaAg** and **DyAg**. R, Raman active mode; I, Infrared active mode.

LaAg				DyAg			
Mode *a*	**Frequency [THz]**	**Irreducible representation**	**Infrared intensity**	**Mode *b***	**Frequency [THz]**	**Irreducible representation**	**Infrared intensity**
1	0.777	E_{2u}	0	1	0.820	E_{2u}	0
2	0.777	E_{2u}	0	2	0.820	E_{2u}	0
3	0.969	E_{2g}(R)	0	3	**1.095**	**E_{1u}(I)**	**0.00448904**
4	0.969	E_{2g}(R)	0	**4**	**1.125**	**Mixture of 7 A_{2u}(I) + 15 E_{1u}(I)**	**0.00023282**
5	**1.024**	**E_{1u}(I)**	**0.00157241**	**5**	1.147	E_{2g}(R)	0
6	**1.035**	**Mixture of 9 A_{2u}(I) + 15 E_{1u}(I)**	**0.00006621**	6	1.147	E_{2g}(R)	0
7	1.111	B_{1u}	0	7	1.195	B_{1u}	0
8	1.161	Mixture of 9 A_{2u}(I) + 15 E_{1u}(I)	0.00000085	8	1.212	E_{1u}(I)	0.00000093
9	1.181	E_{2u}	0	9	1.212	Mixture of 7 A_{2u}(I) + 15 E_{1u}(I)	0.00000001
10	1.181	E_{2u}	0	10	1.218	E_{2u}	0
11	1.205	E_{1u}(I)	0.00202431	11	1.218	E_{2u}	0
12	1.213	Mixture of 9 A_{2u}(I) + 15 E_{1u}(I)	0.00013444	12	1.262	Mixture of 7 A_{2u}(I) + 15 E_{1u}(I)	0.00000013
13	1.414	B_{2u}	0	13	1.323	B_{2u}	0
14	1.416	A_{1u}	0	14	1.425	A_{1u}	0
15	1.791	A_{2g}	0	15	1.550	A_{2g}	0
16	1.809	E_{1u}(I)	0.00121035	16	1.827	E_{1u}(I)	0.00068595
17	1.812	Mixture of 9 A_{2u}(I) + 15 E_{1u}(I)	0.00007102	17	1.834	Mixture of 7 A_{2u}(I) + 15 E_{1u}(I)	0.00001734
18	2.086	B_{2u}	0	18	1.835	E_{2g}(R)	0
19	2.126	E_{2g}(R)	0	19	1.835	E_{2g}(R)	0
20	2.126	E_{2g}(R)	0	20	1.960	B_{2u}	0
21	2.801	B_{1g}	0	21	2.888	E_{2u}	0
22	2.917	E_{2u}	0	22	2.888	E_{2u}	0
23	2.917	E_{2u}	0	23	3.045	E_{1g}(R)	0
24	2.933	E_{1g}(R)	0	24	3.045	E_{1g}(R)	0
25	2.933	E_{1g}(R)	0	25	3.331	E_{1u}(I)	0.00508052
26	3.105	E_{1g}(R)	0	26	3.333	B_{1u}	0
27	3.105	E_{1g}(R)	0	27	3.340	Mixture of 7 A_{2u}(I) + 15 E_{1u}(I)	0.00021019
28	3.169	B_{2g}	0	28	3.372	B_{2g}	0
29	3.364	E_{1u}(I)	0.01749503	29	3.568	E_{2u}	0
30	3.390	A_{1u}	0	30	3.568	E_{2u}	0
31	3.404	Mixture of 9 A_{2u}(I) + 15 E_{1u}(I)	0.00048731	31	3.763	B_{1g}	0
32	3.510	E_{2u}	0	32	3.955	E_{1g}(R)	0
33	3.510	E_{2u}	0	33	3.955	E_{1g}(R)	0
34	3.571	Mixture of 9 A_{2u}(I) + 15 E_{1u}(I)	0.00000719	34	4.421	Mixture of 7 A_{2u}(I) + 15 E_{1u}(I)	0.00004429
35	3.618	B_{1u}	0	35	4.459	E_{2g}(R)	0
36	3.835	E_{2u}	0	36	4.459	E_{2g}(R)	0
37	3.835	E_{2u}	0	37	4.481	A_{1u}	0
38	4.021	E_{2g}(R)	0	38	4.507	E_{2u}	0
39	4.021	E_{2g}(R)	0	39	4.507	E_{2u}	0
40	4.215	B_{2g}	0	40	4.527	B_{2g}	0
41	4.407	A_{2g}	0	41	4.838	A_{2u}(I)	0.00001147
42	4.656	E_{1u}(I)	0.27284017	42	4.892	E_{1u}(I)	0.31732286
43	4.768	E_{2g}(R)	0	43	5.287	A_{2g}	0
44	4.768	E_{2g}(R)	0	44	5.343	E_{2g}(R)	0
45	4.822	A_{1g}(R)	0	45	5.343	E_{2g}(R)	0
46	4.913	B_{2u}	0	46	5.565	A_{1g}(R)	0

47	5.138	Mixture of 9 A_{2u}(I) + 15 E_{1u}(I)	0.00594237	47	5.594	Mixture of 7 A_{2u}(I) + 15 E_{1u}(I)	0.0219624
48	5.235	Mixture of 9 A_{2u}(I) + 15 E_{1u}(I)	0.00000039	48	6.018	B_{2u}	0
49	5.303	E_{1u}(I)	0.03453500	49	6.146	E_{1u}(I)	0.00078289
50	5.382	B_{1u}	0	50	6.148	Mixture of 7 A_{2u}(I) + 15 E_{1u}(I)	0.00020291
51	5.567	Mixture of 9 A_{2u}(I) + 15 E_{1u}(I)	0.02001846	51	6.279	B_{1u}	0
52	6.178	E_{1g}(R)	0	52	6.608	E_{1g}(R)	0
53	6.178	E_{1g}(R)	0	53	6.608	E_{1g}(R)	0
54	6.608	B_{2g}	0	54	6.804	B_{2g}	0
55	6.611	E_{2u}	0	55	7.048	Mixture of 7 A_{2u}(I) + 15 E_{1u}(I)	0.00000008
56	6.611	E_{2u}	0	56	7.174	E_{2u}	0
57	6.785	Mixture of 9 A_{2u}(I) + 15 E_{1u}(I)	0.00000017	57	7.174	E_{2u}	0
58	7.603	E_{1g}(R)	0	58	8.051	E_{2g}(R)	0
59	7.603	E_{1g}(R)	0	59	8.051	E_{2g}(R)	0
60	7.678	B_{1g}	0	60	8.222	E_{1u}(I)	0.02705785
61	7.704	E_{2g}(R)	0	61	8.255	Mixture of 7 A_{2u}(I) + 15 E_{1u}(I)	0.00125305
62	7.704	E_{2g}(R)	0	62	8.290	E_{1g}(R)	0
63	7.791	B_{2g}	0	63	8.290	E_{1g}(R)	0
64	8.004	A_{2g}	0	64	8.314	A_{1g}(R)	0
65	8.032	A_{1g}(R)	0	65	8.437	B_{1u}	0
66	8.042	E_{2g}(R)	0	66	8.503	E_{2g}(R)	0
67	8.042	E_{2g}(R)	0	67	8.503	E_{2g}(R)	0
68	8.230	E_{1g}(R)	0	68	8.674	B_{1g}	0
69	8.230	E_{1g}(R)	0	69	8.839	B_{2g}	0
70	8.754	Mixture of 9 A_{2u}(I) + 15 E_{1u}(I)	0.00037298	70	9.139	A_{1g}(R)	0
71	8.754	E_{1u}(I)	0.00001530	71	9.206	E_{1g}(R)	0
72	8.772	E_{2g}(R)	0	72	9.206	E_{1g}(R)	0
73	8.772	E_{2g}(R)	0	73	9.206	A_{2g}	0
74	8.998	E_{1u}(I)	0.09915326	74	9.254	E_{2g}(R)	0
75	9.021	E_{2u}	0	75	9.254	E_{2g}(R)	0
76	9.021	E_{2u}	0	76	9.396	E_{1u}(I)	0.48535661
77	9.040	A_{1g}(R)	0	77	9.564	E_{2u}	0
78	9.090	B_{1u}	0	78	9.564	E_{2u}	0
79	9.132	Mixture of 9 A_{2u}(I) + 15 E_{1u}(I)	0.00808442	79	9.756	Mixture of 7 A_{2u}(I) + 15 E_{1u}(I)	0.00002524
80	9.203	Mixture of 9 A_{2u}(I) + 15 E_{1u}(I)	0.00003587	80	9.769	E_{2u}	0
81	9.400	B_{1u}	0	81	9.769	E_{2u}	0
82	9.728	A_{1u}	0	82	9.829	Mixture of 7 A_{2u}(I) + 15 E_{1u}(I)	0.00685972
83	9.843	E_{2u}	0	83	9.931	E_{2g}(R)	0
84	9.843	E_{2u}	0	84	9.931	E_{2g}(R)	0
85	9.887	B_{2u}	0	85	9.947	E_{1u}(I)	0.06675043
86	9.972	E_{1u}(I)	0.01077787	86	9.974	B_{1u}	0
87	9.987	Mixture of 9 A_{2u}(I) + 15 E_{1u}(I)	0.00078244	87	10.172	E_{1g}(R)	0
88	10.061	E_{1g}(R)	0	88	10.172	E_{1g}(R)	0
89	10.061	E_{1g}(R)	0	89	10.225	A_{1u}	0
90	10.137	E_{2u}	0	90	10.415	Mixture of 7 A_{2u}(I) + 15 E_{1u}(I)	0.04644216
91	10.137	E_{2u}	0	91	10.538	B_{2u}	0
92	11.308	E_{2g}(R)	0	92	10.590	E_{1u}(I)	0.01003036
93	11.308	E_{2g}(R)	0	93	10.670	Mixture of 7 A_{2u}(I) + 15 E_{1u}(I)	0.02952553
94	11.317	E_{1u}(I)	0.48995740	94	10.684	E_{2u}	0
95	12.021	Mixture of 9 A_{2u}(I) + 15 E_{1u}(I)	0.06766835	95	10.684	E_{2u}	0
96	12.710	E_{1g}(R)	0	96	11.602	E_{1g}(R)	0
97	12.710	E_{1g}(R)	0	97	11.602	E_{1g}(R)	0
98	12.711	E_{2g}(R)	0	98	11.695	E_{2g}(R)	0
99	12.711	E_{2g}(R)	0	99	11.695	E_{2g}(R)	0
100	12.930	B_{2g}	0	100	11.842	B_{2g}	0
101	13.525	A_{1g}(R)	0	101	12.473	E_{2u}	0
102	13.564	E_{1u}(I)	0.05923220	102	12.473	E_{2u}	0
103	13.579	E_{2u}	0	103	12.540	E_{1u}(I)	0.05403404
104	13.579	E_{2u}	0	104	12.559	Mixture of 7 A_{2u}(I) + 15 E_{1u}(I)	0.00015071
105	13.582	Mixture of 9 A_{2u}(I) + 15 E_{1u}(I)	0.00005539	105	12.593	A_{1g}(R)	0
106	13.707	Mixture of 9 A_{2u}(I) + 15 E_{1u}(I)	0.01868054	106	12.669	Mixture of 7 A_{2u}(I) + 15 E_{1u}(I)	0.01658371
107	13.875	B_{1g}	0	107	13.089	B_{1u}	0

108	13.881	A_{1u}	0	108	13.518	B_{1g}	0
109	14.070	B_{1u}	0	109	13.535	A_{1u}	0
110	14.527	B_{2g}	0	110	14.279	Mixture of 7 A_{2u}(I) + 15 E_{1u}(I)	0.00003327
111	14.553	Mixture of 9 A_{2u}(I) + 15 E_{1u}(I)	0.00009024	111	14.320	B_{2g}	0
112	14.891	E_{2u}	0	112	14.757	E_{2u}	0
113	14.891	E_{2u}	0	113	14.757	E_{2u}	0
114	14.905	E_{1g}(R)	0	114	14.770	E_{1g}(R)	0
115	14.905	E_{1g}(R)	0	115	14.770	E_{1g}(R)	0
116	16.805	B_{2u}	0.00000000	116	15.741	B_{2u}	0
117	16.806	A_{2g}	0	117	15.743	A_{2g}	0
118	47.552	B_{1u}	0	118	47.256	B_{1u}	0
119	47.556	A_{1g}(R)	0	119	47.256	A_{1g}(R)	0
120	47.656	E_{1u}(I)	0.02717143	120	47.325	E_{1u}(I)	0.24538358
121	47.666	E_{2g}(R)	0	121	47.330	E_{2g}(R)	0
122	47.666	E_{2g}(R)	0	122	47.330	E_{2g}(R)	0
123	47.727	Mixture of 9 A_{2u}(I) + 15 E_{1u}(I)	0.02833955	123	47.424	Mixture of 7 A_{2u}(I) + 15 E_{1u}(I)	0.03222367
124	65.678	E_{2u}	0	124	65.225	E_{2u}	0
125	65.678	E_{2u}	0	125	65.225	E_{2u}	0
126	65.682	E_{1u}(I)	0.22578270	126	65.243	A_{2u}(I)	0.00060314
127	65.712	Mixture of 9 A_{2u}(I) + 15 E_{1u}(I)	0.00424163	127	65.243	E_{1u}(I)	0.17311797
128	65.736	Mixture of 9 A_{2u}(I) + 15 E_{1u}(I)	0.03356660	128	65.285	Mixture of 7 A_{2u}(I) + 15 E_{1u}(I)	0.02325628
129	66.013	B_{2g}	0	129	65.498	B_{2g}	0
130	66.030	E_{1g}(R)	0	130	65.511	E_{1g}(R)	0
131	66.030	E_{1g}(R)	0	131	65.511	E_{1g}(R)	0
132	66.037	E_{2g}(R)	0	132	65.528	E_{2g}(R)	0
133	66.037	E_{2g}(R)	0	133	65.528	E_{2g}(R)	0
134	66.071	B_{1u}	0	134	65.547	B_{1u}	0
135	66.273	A_{1g}(R)	0	135	65.722	A_{1g}(R)	0
136	106.226	E_{1u}(I)	1.05644929	136	107.561	E_{1u}(I)	0.84091332
137	106.237	E_{2g}(R)	0	137	107.568	E_{2g}(R)	0
138	106.237	E_{2g}(R)	0	138	107.568	E_{2g}(R)	0
139	106.385	Mixture of 9 A_{2u}(I) + 15 E_{1u}(I)	0.13335259	139	107.670	Mixture of 7 A_{2u}(I) + 15 E_{1u}(I)	0.10922289
140	106.452	A_{1g}(R)	0	140	107.726	B_{1u}	0.00000002
141	106.454	B_{1u}	0.00000004	141	107.727	A_{1g}(R)	0
142	107.992	E_{2u}	0	142	109.695	E_{2u}	0
143	107.992	E_{2u}	0	143	109.695	E_{2u}	0
144	108.007	E_{1g}(R)	0	144	109.704	E_{1g}(R)	0
145	108.007	E_{1g}(R)	0	145	109.704	E_{1g}(R)	0
146	108.146	Mixture of 9 A_{2u}(I) + 15 E_{1u}(I)	0.00006199	146	109.817	Mixture of 7 A_{2u}(I) + 15 E_{1u}(I)	0.00002853
147	108.227	B_{2g}	0	147	109.886	B_{2g}	0

Table S6. Table of irreducible representations of point group D_{6h} (6*/mmm*). R, Raman active mode; I, Infrared active mode.

irreducible representations	**1**	**6**	**5**	**2**	**3**	**4**	**9**	**8**	**7**	**10**	**12**	**11**	
A_{1g}(R)	1	1	1	1	1	1	1	1	1	1	1	1	x^2+y^2
A_{2g}	1	1	1	1	1	1	-1	-1	-1	-1	-1	-1	
B_{1g}	1	-1	-1	1	1	-1	1	1	1	-1	-1	-1	
B_{2g}	1	-1	-1	1	1	-1	-1	-1	-1	1	1	1	
E_{1g}(R)	2	1	1	-1	-1	-2	0	0	0	0	0	0	(xz,yz)
E_{2g}(R)	2	-1	-1	-1	-1	2	0	0	0	0	0	0	(x^2-y^2,xy)
A_{1u}	1	1	1	1	1	1	1	1	1	1	1	1	
A_{2u}(I)	1	1	1	1	1	1	-1	-1	-1	-1	-1	-1	z
B_{1u}	1	-1	-1	1	1	-1	1	1	1	-1	-1	-1	
B_{2u}	1	-1	-1	1	1	-1	-1	-1	-1	1	1	1	
E_{1u}(I)	2	1	1	-1	-1	-2	0	0	0	0	0	0	(x,y)
E_{2u}	2	-1	-1	-1	-1	2	0	0	0	0	0	0	
irreducible representations	**13**	**18**	**17**	**14**	**15**	**16**	**21**	**20**	**19**	**22**	**24**	**23**	
A_{1g}(R)	1	1	1	1	1	1	1	1	1	1	1	1	x^2+y^2
A_{2g}	1	1	1	1	1	1	-1	-1	-1	-1	-1	-1	
B_{1g}	1	-1	-1	1	1	-1	1	1	1	-1	-1	-1	
B_{2g}	1	-1	-1	1	1	-1	-1	-1	-1	1	1	1	
E_{1g}(R)	2	1	1	-1	-1	-2	0	0	0	0	0	0	(xz,yz)
E_{2g}(R)	2	-1	-1	-1	-1	2	0	0	0	0	0	0	(x^2-y^2,xy)
A_{1u}	-1	-1	-1	-1	-1	-1	-1	-1	-1	-1	-1	-1	
A_{2u}(I)	-1	-1	-1	-1	-1	-1	1	1	1	1	1	1	z
B_{1u}	-1	1	1	-1	-1	1	-1	-1	-1	1	1	1	
B_{2u}	-1	1	1	-1	-1	1	1	1	1	-1	-1	-1	
E_{1u}(I)	-2	-1	-1	1	1	2	0	0	0	0	0	0	(x,y)
E_{2u}	-2	1	1	1	1	-2	0	0	0	0	0	0	

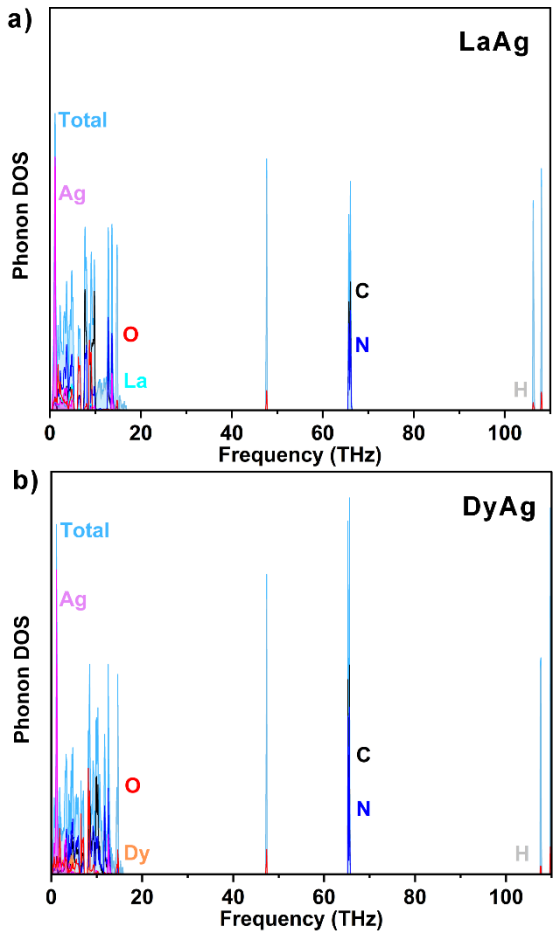

Figure S13. Total phonon density of states (DOS) in light blue colored peak of the **LaAg** (a) and **DyAg** (b) and partial phonon DOS of La, cyan line; Dy, orange line; Ag, pink colored peak; O, red line; C, black line; N, blue line; H, grey line.

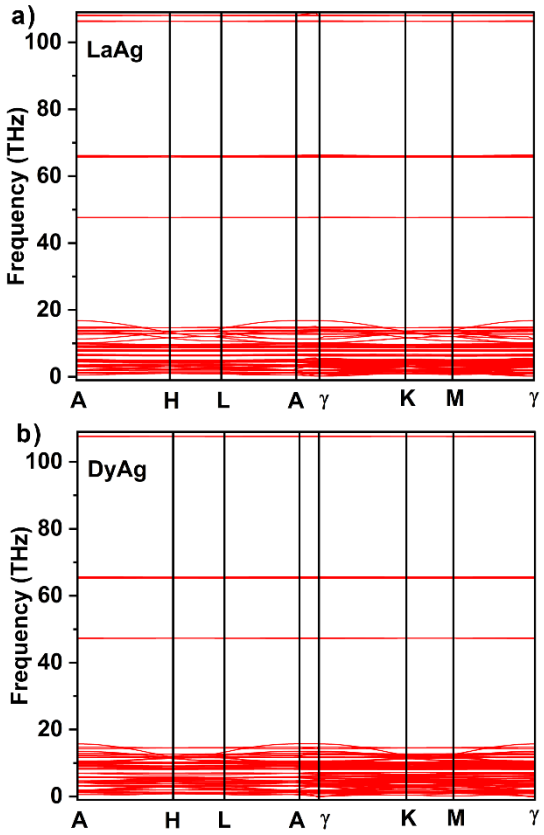

Figure S14. Phonon dispersion of **LaAg** (a) and **DyAg** (b).

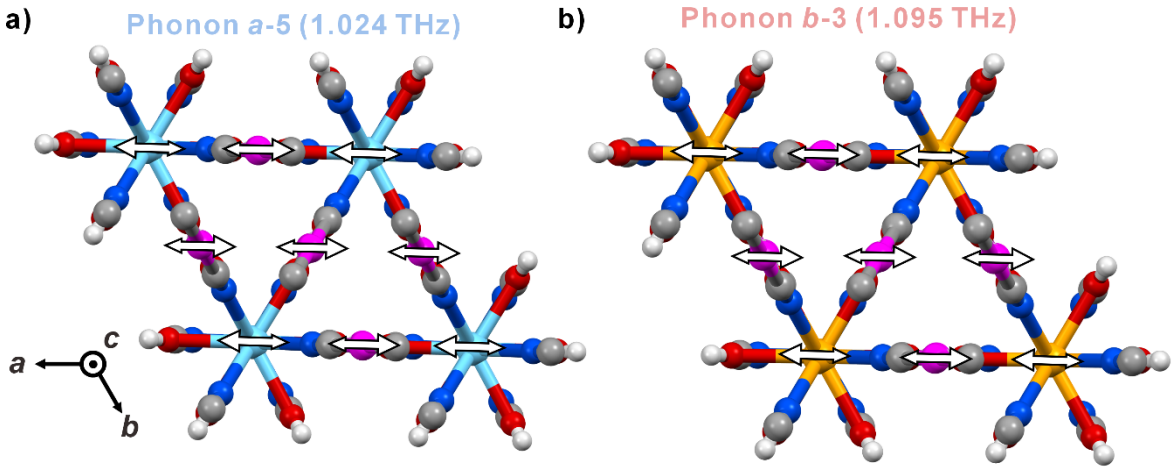

Figure S15. Atomic motion projections of the phonon modes for two phonon modes *a*-6 and *b*-4 along the *c*-axis. Color: La, cyan; Dy, orange; Ag, pink; C, dark gray; N, blue; O, red; H, light gray. The arrows indicate the vibration vectors.